12-1-2004

Experimental and Analytical Study of a Retrofitted Pin and Hanger Bridge

Robert J. Connor

Bridget Webb

Ian C. Hodgson

Carl A. Bowman

EXPERIMENTAL AND ANALYTICAL STUDY OF A RETROFITTED PIN AND HANGER BRIDGE

Final Report

by

Robert J. Connor
Bridget Webb
Ian C. Hodgson
Carl A. Bowman

ATLSS Report No. 04-02

January 2004

ATLSS is a National Center for Engineering Research on Advanced Technology for Large Structural Systems

117 ATLSS Drive
Bethlehem, PA 18015-4729

Phone: (610)758-3525
Fax: (610)758-5902

www.atlss.lehigh.edu
Email: fieldtesting@lehigh.edu

EXPERIMENTAL AND ANALYTICAL STUDY OF A RETROFITTED PIN AND HANGER BRIDGE

Robert J. Connor
Research Engineer
ATLSS Engineering Research Center

Bridget Webb
Undergraduate Research Assistant

Ian C. Hodgson
Research Engineer
ATLSS Engineering Research Center

Carl A. Bowman
Instrumentation Technician
ATLSS Engineering Research Center

ATLSS Report No. 04-02

January 2004

ATLSS is a National Center for Engineering Research on Advanced Technology for Large Structural Systems

117 ATLSS Drive
Bethlehem, PA 18015-4729

Phone: (610)758-3525
Fax: (610)758-5902

www.atlss.lehigh.edu
Email: fieldtesting@lehigh.edu

Table of Contents

1.0 Project Summary

In July 1983, a two-girder pin and hanger bridge carrying I-95 over the Mianus River collapsed in Greenwich, CT when a pin and hanger system failed [1]. This collapse spurred studies of this bridge type including a PennDOT investigation of all fracture-critical bridges with pin and hanger connections. Many owners required retrofit of these bridges in order to provide more redundancy for a greater level of safety. Retrofits ranged from systems intended to "catch" the suspended span should a portion of the linkage fail, to complete replacement of the pin and hanger with a fully bolted girder splice.

The objective of this project is to study the behavior of one bridge in which the latter retrofit strategy was employed and calibrate a finite element model of the existing bridge to accurately estimate the behavior of the original pin and hanger design.

2.0 Background

2.1 Pin and Hanger Systems

Pin and hanger connections were used in bridges primarily to simplify analyses since the calculations were primarily performed using hand methods. Continuous multi-span bridge structures were difficult to analyze and required tedious calculations in order to estimate live load shear and moment envelopes. Pin and hanger systems were also found to be useful in accommodating longitudinal expansion as well as avoiding corrosion by reducing the number of deck joints and moving the necessary joints away from the bearings.

The concept behind most pin and hanger systems is to suspend one section of the bridge from two anchor sections by way of the pin and hanger connection. One pin would be located on the end of each girder. The adjacent girders were then connected by the hangers as shown in Figure 1 and Appendix A.

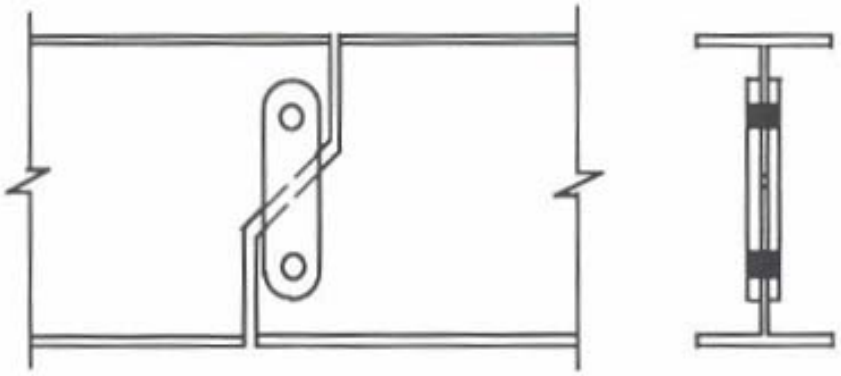

Figure 1 – Pin and hanger schematic, elevation and cross section [2]

2.2 Redundancy Theory and Other Issues

Redundant structures provide alternate load paths in the event of the failure of a primary load carrying member. A structure is considered to be non-redundant if the failure of one of the primary load carrying members would result in collapse or failure of the structure. Typically, the failure mode of the member is often considered to be fracture of a tension member. However, buckling failure of a primary compression member, such as found in a cantilevered truss, can also result in failure of the structure. Fracture critical members are those whose failure by brittle fracture would lead to collapse of the bridge. A relatively new term introduced in the AASHTO LRFD refers to a failure critical member and describes a member whose failure would lead to collapse of the bridge. The failure mode could be fracture or any other failure mode. Hence, although fracture critical members are considered failure critical, the converse is not true.

The bridge under study could be considered doubly non-redundant in the as-designed condition as it contained both the pin and hanger connections and was supported by a two-girder superstructure. Pin and hanger systems are considered fracture-critical members as they are non-redundant members loaded in tension. For example, fracture of the linkage would be expected to result in collapse of the bridge. If the tension flange of one of the two girders were to fracture, no alternate load path would exist to avoid collapse thereby making the two-girder system non-redundant [3].

2.3 Description of Bridge

The Clarks Summit Bridge is a two-girder, riveted steel bridge as shown in Figure 2. The total length is 1626'-10" consisting of eight main spans of 170'-3" and two end spans of 132'-5". It has a maximum clearance of 139'-5". The bridge is located at the northernmost end of the northeast extension of the Pennsylvania Turnpike in Clarks Summit, PA and crosses over U.S. Routes 6 and 11, D.L. and W.R.R., and Abington Boulevard. The bridge was designed in 1955 and built shortly thereafter.

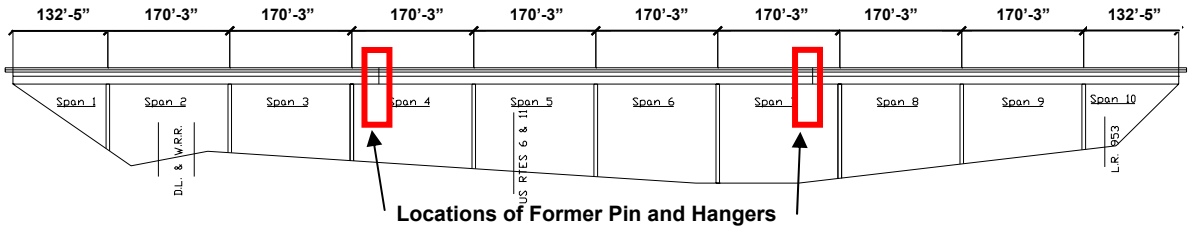

Figure 2 – Elevation view of Clarks Summit Bridge

2.4 Original Design

The original design consisted of one multi-span center section and two multi-span approach sections. Spans four and seven each contained pin and hangers on each girder as shown in Figure 2. Each of the pin and hanger joints theoretically acted as a zero-moment connection. The center-to-center distance between the pins was 7'-10 ½" and the nominal area of the each hanger was 21.0 in^2.

2.5 Details of the Retrofit

During a routine field inspection, a hairline crack was found on one of the hangers which lead to an emergency closure of the bridge. For safety reasons, all four of the pin and hanger systems were replaced with a full-girder splice. At each joint, approximately 9'-4" of the girder was removed on each side of the joint and replaced with a continuous length of girder which was bolt-spliced in place. The new section of girder was fabricated using bolted built-up plates and angles into a plate girder that matched the original riveted girders. After the retrofit, the bridge was continuous from end to end. All expansion was accommodated with finger joints at the abutments.

3.0 Finite Element Analysis

A simple finite element analysis of both the as-designed (with the pin and hangers) and retrofitted (without the pin and hangers) structure was performed using SAP 2000 Plus. Various two-dimensional line-girder models were created for combinations of composite and non-composite sections; and variable and constant girder section properties. Separate models were developed of the retrofitted structure to investigate the contribution of the slab assuming full composite action and compared to non-composite models. In addition, as a small pilot study, a model was created in which the steel section properties of the entire girder (i.e., all ten spans) were kept constant (i.e., the steel section was held constant). This analysis was performed in order to establish the influence of the change in section along the length of the girder on the distribution of moment and shear throughout the structure.

One model was created using the variable section properties steel girder composite with the deck for the as-designed structure. Moment envelopes and moment influence lines were developed using a moving point load analysis. All models were loaded with a single 100 kip moving load to simulate a truck driving across the bridge. All influence line models were generated with a single one-kip moving load. Using these data, stress influence lines were developed in order to compare with the field measurements.

3.1 Analysis of Variable Sections

The girders of the Clarks Summit Bridge are riveted built-up girders. The steel section varies along the length of the girder due to the addition of coverplates, as well as variations in the web plate thickness. The girder cross section is greatest over the piers and in the positive moment region of each span. As discussed, models with a constant steel cross section and variable steel cross section were created. The two were compared with the objective of determining if a non-variable section moduli would provide a reasonable estimate of the behavior of the bridge.

As shown in Figures 3 and 4, the moment envelopes of the two models were identical in shape. (*Figures 3 and 4 only show half of the model since the bridge is symmetric*). There were, however, small differences in the magnitude of the moment at

any point along the envelope. The maximum positive and negative moments obtained from the moment envelopes are presented in Figures 3 and 4. A shift of approximately 15% occurred. Thus, for a quick estimate of the location of positive and negative moment regions, using a constant cross section will yield reasonable results.

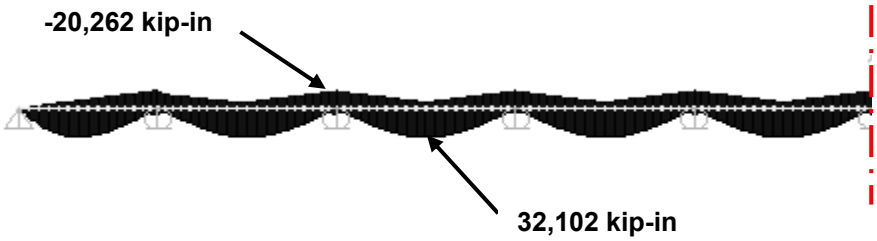

Figure 3 – Moment envelope for variable-section, non-composite model (half length)

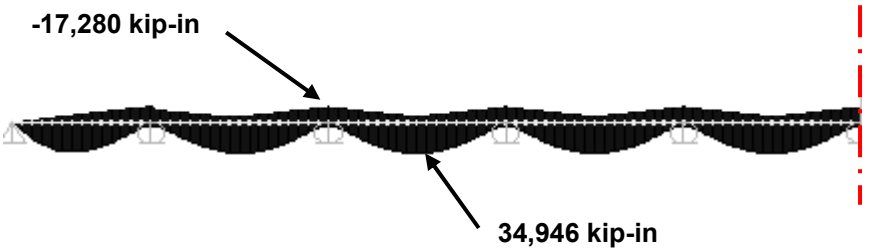

Figure 4 – Moment envelope for non-variable-section, non-composite model (half length)

According to the American Institute of Steel Construction (AISC) handbook of moments, shears, and reactions, a 50% increase in moment of inertia of the steel section over the pier will produce a 5% increase in negative moment (*i.e., a downward shift of 5%*) [5]. The moment of inertia increase over pier 3 was about 112% from the base or lightest girder cross section due solely to the addition of coverplates. Assuming linear behavior, one would estimate the shift in the moment diagram to be about 11.2%. However, according to the AISC handbook, the increase should be greater than 11.2% as the relationship is non-linear. The actual downward shift was about 15% and seems reasonable, considering the magnitude of the variation in cross section.

3.2 Analysis of Composite Girder and Deck

The bridge was initially designed with a non-composite cast-in-place reinforced concrete deck and was later redecked using pre-cast deck panels assuming non-composite action in 1979. Models were created for both the composite and non-composite cases for each of the variable and constant cross section cases. Overall, there was no difference between the composite and non-composite cases for the constant section models. The distribution of moment along the girder was identical as expected.

Composite action caused the moment envelope for the model with a variable steel cross section to be shifted downward approximately 10% from the moment envelope of the non-composite variable section. Hence, considering composite action resulted in an overall decrease in the moment in the girders as expected.

3.3 Analysis of Moment at Former Pin and Hanger Connection

Three FE models were created of the bridge assuming different structural configurations, as shown in Figures 5 through 7. The first model (Figure 5) simulated the bridge as it was originally designed including the pin and hanger connections. The other two models simulated the bridge after the pin and hangers were removed. Both included the variable steel cross section; one with composite action (Figure 6), the other, non-composite (Figure 7). As shown in Figure 5, the model which represented the as-designed case showed a zero-moment connection at the original pin and hanger joint. Figures 6 and 7, which are of the retrofitted bridge indicate a full-moment connection at the existing spliced joints and nearly identical moment envelopes.

Figure 5 – Moment envelope for pin and hanger model (half length)

Figure 6 – Moment envelope for as retrofitted composite model (half length)

Figure 7 - Moment envelope for as retrofitted non-composite model (half length)

4.0 Field Instrumentation and Data Acquisition

All strain gages were uniaxial weldable gages produced by Measurements Group Inc. and were 0.25 in. gage length type LWK-06-W250B-350 (See Figure 8). A total of 18 gages were installed. Weldable type strain gages were selected due to ease of installation in a variety of weather conditions. The "welds" are a point or spot resistance weld about the size of a pinprick. The probe is powered by a battery and only touches the foil that the strain gage is mounted on by the manufacturer. This fuses a small pin size area to the steel surface. It takes ten or more of these dots to attach the gage to the steel surface. There are no arc strikes or heat affected zones that are discernible. There is no preheat or any other preparation involved other than the preparation of the local metal surface by grinding and then cleaning before the gage is attached to the component with the welding unit. There has never been an instance of adverse behavior associated with the use of weldable strain gages including their installation on extremely brittle material such as A615 Gr75 steel reinforcing bars.

Figure 8 – Typical strain gage installed on bottom flange of a girder

These gages are a temperature-compensated uniaxial strain gage and perform very well when accurate strain measurements are required over long periods of time (months to years). The gage resistance was 350Ω and an excitation voltage of 10 Volts was used. The gages where installed at locations where access was good and the effects of very high strain gradients were not a concern.

Data were recorded using a CR9000 data logger manufactured by Campbell Scientific as shown in Figure 9. The CR9000 is a modular, multi-channel digital data acquisition system that provides precision measurement capabilities in a rugged, battery-operated package. The logger used was powered with two solar panel units and batteries, as shown in Figure 10. Signal wires were run from each of the gages to the top of pier three. The wire was then dropped down pier three to the data logger located at the base of the pier.

In order to establish stress-range histograms, uncontrolled monitoring of all gages was conducted. The monitoring lasted for a period of six days and 22.5 hours. The stress-range histograms were verified by simultaneously collecting triggered time history data for all gages. Data were recorded when stresses reached predefined levels in the bottom flange of the east or west girder in the positive moment region. The magnitudes

were established based the results of the controlled tests and some random traffic data which were collected the day before the uncontrolled monitoring program was started.

For example, assume it was determined that the test truck produces a peak stress of 2.0 ksi in the bottom flange. Software triggers would then be set at about 1.9 ksi for these gages. If the stress exceeds that value, the time history is recorded. Data will also be recorded prior to the trigger event for a specified amount of time, say 5 seconds (i.e., a 5 second buffer will be maintained). The data acquisition system will continue to record for an additional specified time period, again, say 5 seconds and then stop recording. (The channels monitored as triggered time histories were automatically re-zeroed using a digital balance algorithm.)

As stated, stress-range histograms were also developed using the rainflow cycle counting method. The stress-range histograms were generated continuously and did not operate on triggers, thus all cycles are counted. In addition, the histograms were updated every ten minutes. Thus, in the event of a power failure, a minimal amount of data would be lost. The stress-range bins were divided into 0.5 ksi intervals and cycles less than 0.2 ksi were not included.

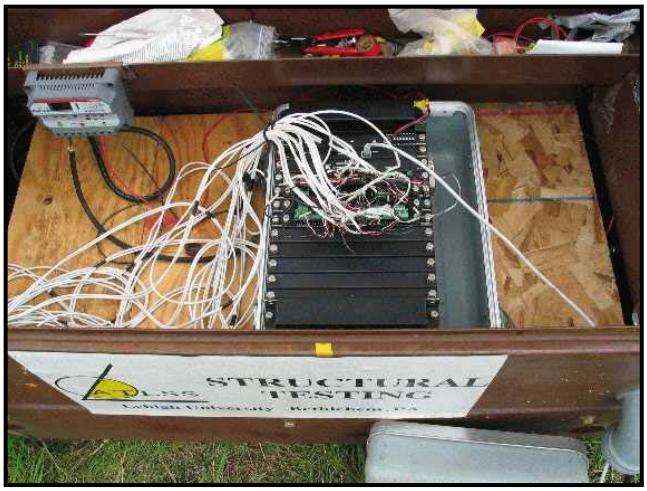

Figure 9 – Photographs of CR9000 data logger installed in weather-tight box

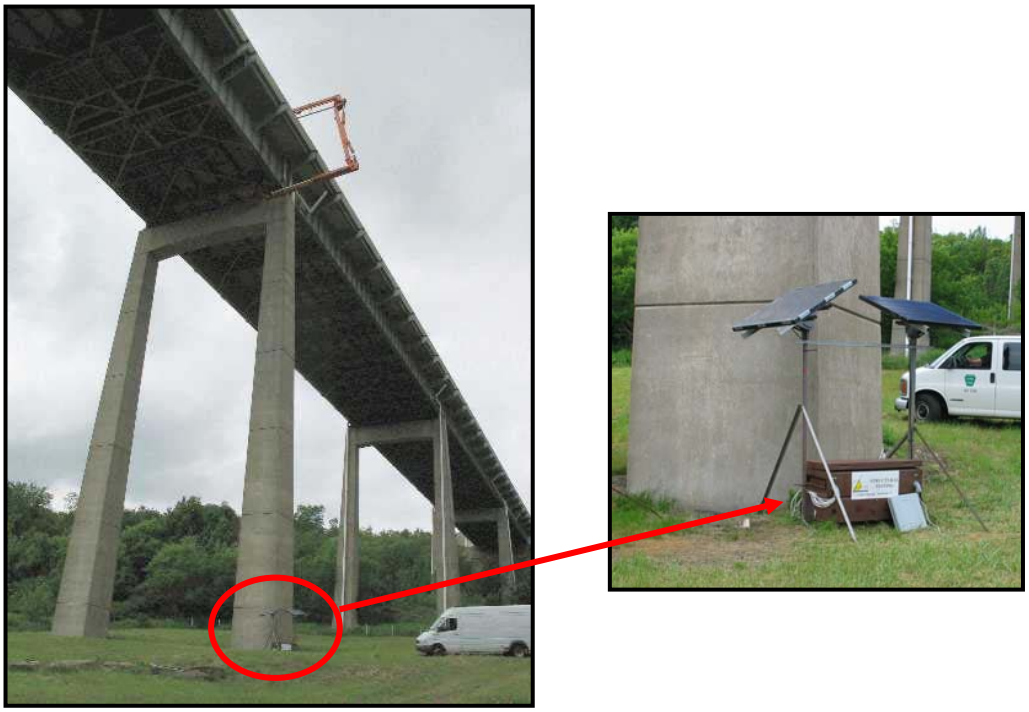

Figure 10 – Data logger and solar panels installed at base of pier three

Using moment envelopes developed by analyzing the variable-section continuous (*i.e., retrofitted*) bridge using SAP 2000, a strain gage plan was developed. Eighteen strain gages were applied as shown in Figure 11. Each girder was instrumented at three locations along the length near pier three. The locations were chosen to include the positive and negative moment regions, as well as the former pin and hanger joint location on each of the main girders in span four. Gages were installed on the bottom of the bottom flange and on the bottom of the top flange. (*Gages could not be installed on the top of the top flange since it was covered by the concrete deck.*)

One floorbeam and one stringer were also instrumented. The floorbeam was instrumented at midspan and near the connection to the main girder to gain some insight into the behavior of this connection. Gages were installed on the top and bottom flange. The first interior stringer under the southbound lanes was selected for instrumentation based on conversations with personnel from the Turnpike who indicated southbound trucks would most likely have a higher GVW than northbound trucks. The strain gage locations can be seen in Figure 11. (*Detailed instrumentation plans are included in Appendix A*) Span four was selected since it previously contained one of the pin and hanger joints and allowed for easy access beneath the bridge providing a convenient location for the data logger.

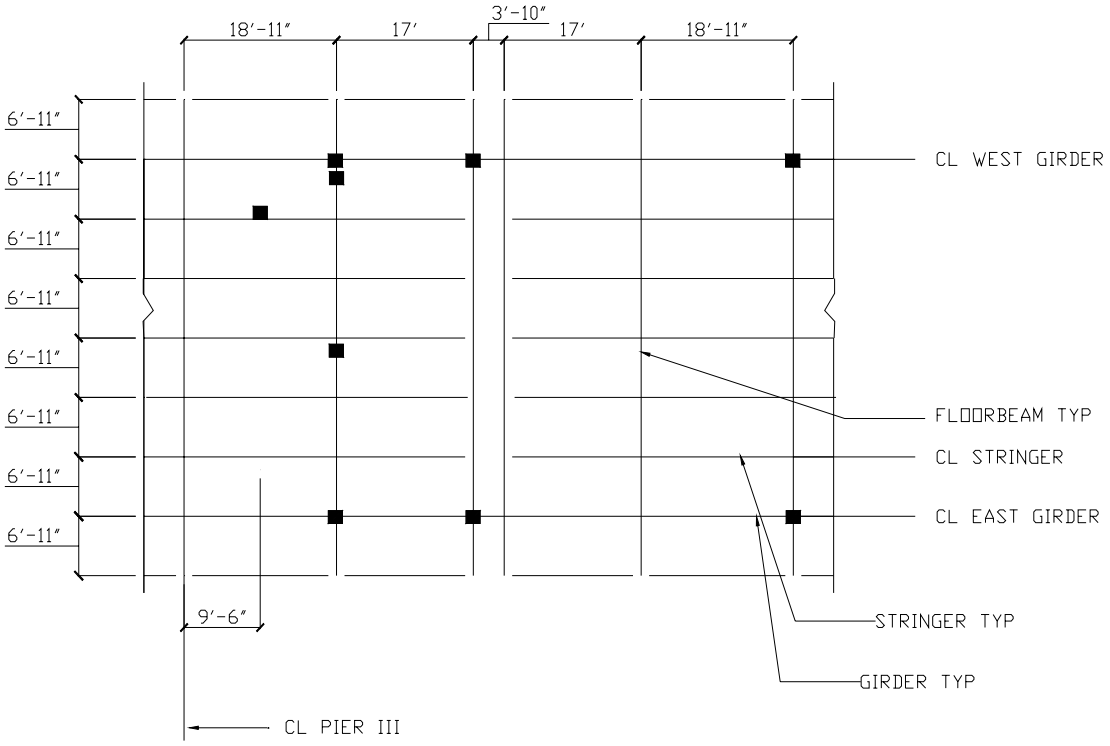

Figure 11 – Instrumentation plan
(*For a detailed strain gage plan see Appendix A*)

5.0 Controlled Load Tests

5.1 Test Truck

The test truck was a four axle Mack Aerial UB 50 snooper with the third rear axle riding up. A photograph of the test truck parked on top of the bridge with the snooper arm extended can be seen in Figure 12. The dimensions of the truck are provided in Figure 13. The steering axle weight was 18,320 pounds; drive axles, 17,580 pounds; trailer axle, 26,540 pounds. The gross vehicle weight of the truck was 62,440 pounds. The truck was provided by the Pennsylvania Turnpike Commission and was labeled as Truck #14-002.

Figure 12 – Photograph of test truck and "snooper"

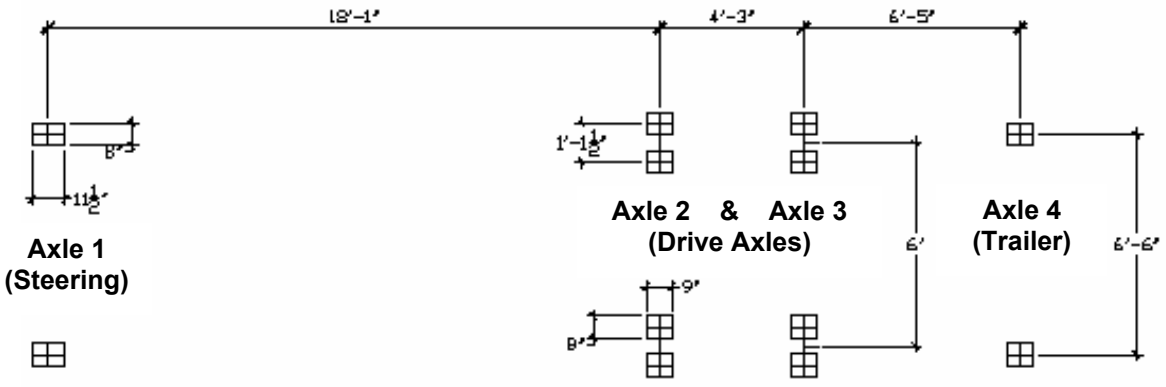

Figure 13 – Dimensions of test truck

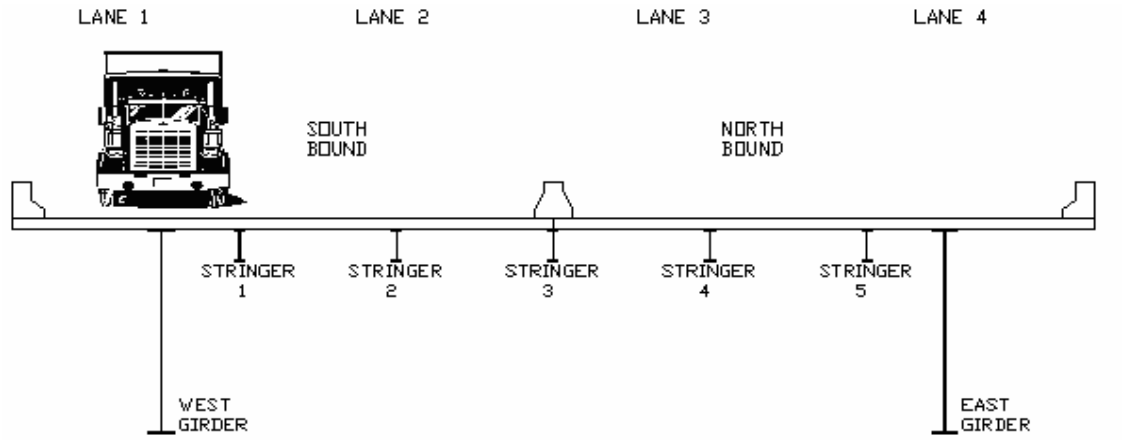

Figure 14 – Location of lane numbers as identified during controlled load testing (View looking northbound)

5.2 Test Program – Summary

Multiple test types were performed and duplicated to establish the variability of the data. Both controlled load tests using a truck of known weight and geometry, and uncontrolled monitoring were conducted. Each test type is described below.

A series of controlled load tests were conducted using a test truck of known load and geometry (See Figure 12). The truck possessed a "floating" third rear axle, which is identified in Figure 13 as the "trailer axle". This rear axle can be lowered using air pressure in order to distribute the rear load to three axles. The third rear axle was in the "up" position for all controlled load tests.

The lane designations used during the controlled load testing can be seen in Figure 14. The tests included crawl, park, and dynamic (speed) tests. During all tests, no other traffic was permitted on the bridge. The crawl tests were performed in each lane twice to establish the variability of the data and determine if the measurements were consistent. Crawl tests were conducted with the truck positioned in each lane and driven slowly (< 5 mph) across the entire bridge. Dynamic forces may be developed due to the moving traffic. However, these effects can only be accurately determined by first establishing the response of the structure to static loads. Therefore the series of crawl tests were conducted prior to conducting the dynamic speed tests. This data is also very useful for comparison to analytical models if developed. The first set of tests in lanes 1 and 4 were recorded separately. For ease of traffic control, the remaining tests were performed as loops, with the southbound test performed first.

Park tests were also conducted. The park tests were performed in lanes 1 and 2 over the instrumented floorbeam with the tires of one side of the truck centered on the instrumented stringer. The outside lane park test consisted of positioning and holding the truck at four positions along the lane. First, the front axle was parked over the first floorbeam south of mid-span. Then, the rear axle was positioned over the same location. These two positions were duplicated over the instrumented floorbeam. The inside lane park test was run with rear axles first on the instrumented floorbeam, then rear axles at the mid-span position. The summary of tests can be seen in Table 1.

Dynamic tests were conducted with the truck in lane 1 and driven southbound. Due to the symmetric response of the bridge observed during the crawl tests, it was decided to only conduct dynamic tests in the southbound direction. Since the greatest stresses in the main girders are produced with the truck in the lane 1 (or lane 4 headed northbound), tests were only conducted in this travel lane.

Test Name	Travel Direction	Lane	Speed (mph)	Comments
SBCRL1_1.dat	Southbound	1	5	Crawl test
NBCRL4_1.dat	Northbound	4	5	Crawl test
SNCRL14.dat	Southbound then Northbound	1 then 4	5	Crawl test duplicate
SNCRL231.dat	Southbound then Northbound	2 then 3	5	Crawl test
SNCRL232.dat	Southbound then Northbound	2 then 3	5	Crawl test duplicate
PARK_1.dat	Southbound	1	---	Park test
PARK_2.dat	Southbound	2	---	Park test
SBL1_D1.dat	Southbound	1	35	Dynamic test
SBL1_D2.dat	Southbound	1	43	Dynamic test duplicate

Table 1 – Summary of controlled load tests using test truck.

5.3 Results of Controlled Load Testing

As previously stated, each of the controlled load tests was repeated in order to ascertain the variability associated with the behavior of the structural system. The data were found to be consistent and repeatable. A maximum variance of 10% was observed in the main girder strain response. There was a maximum variance of 15% in the floorbeam strain response for these tests. Greater variance such as this is to be expected in the floorbeam and stringers. This is directly due to the greater sensitivity of the floorbeam and stringer to transverse position of the test truck. Figure 15 shows the low level of variability in the gage located on the bottom flange of the west-girder at the former pin and hanger joint location during southbound crawl testing in the outside lanes. Although not presented, similar results were observed for all gages and all lane positions.

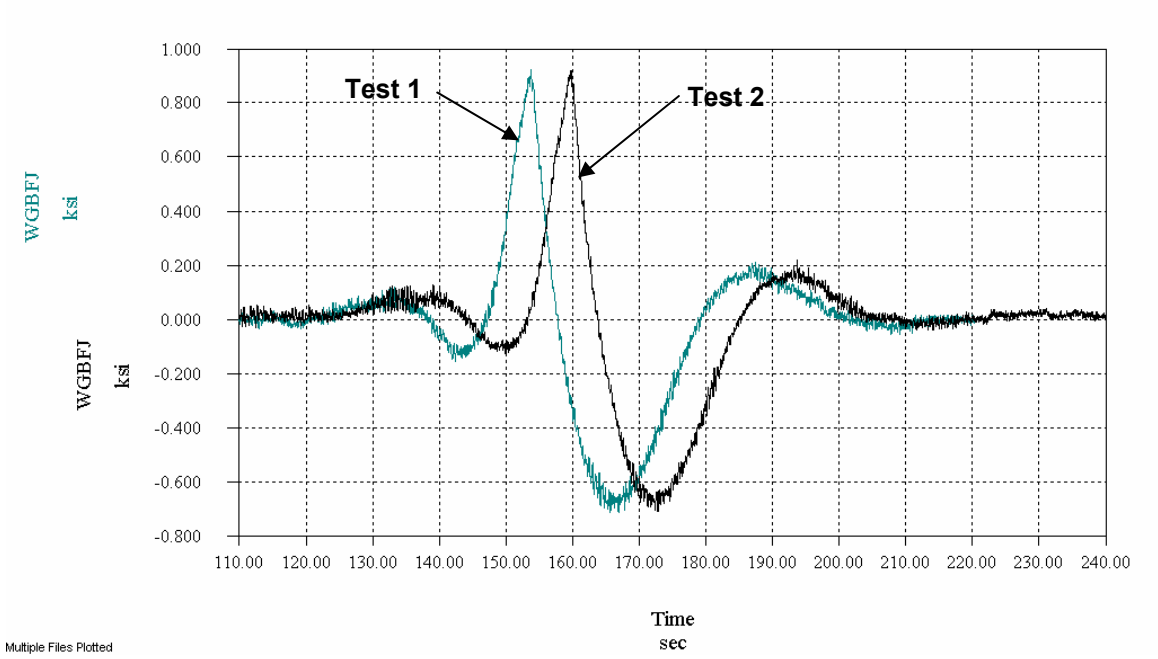

Figure 15 – Comparison of bottom flange response at former pin and hanger location from identical tests with test truck positioned in lane 1 headed southbound

5.4 Main Girder Response

The results of measurements made on the main girders are presented in this section.

5.4.1 Load Distribution in Girders

Two park tests were used to determine the load distribution between the girders. One test was performed with the truck in the outside southbound lane (lane 1). The other was performed with the test truck located in the inside southbound lane (lane 2).

The distribution factors were calculated at points when the stress in the bottom flange was maximum. The bottom flange gages were used due to their higher response to the test load. The data were then normalized and compared with a theoretical distribution factor determined using the lever rule between main girders. The results are presented in Tables 2 and 3. As shown in Table 2, the average distribution factor with the truck in lane 1 matches well with the theoretical distribution factor for both girders. There is some variation with the longitudinal position of the truck however. There is also much poorer agreement when the truck is located in lane 2. The average distribution factors for the east girder with the truck in lane two are in error by about 50%.

The reasons for the error are not exactly known, however it is most likely due to the simple assumptions in calculating the distribution factor using the lever rule. When the truck is in lane one (or four) it is essentially directly over the girder. Hence, most of the load is directly carried by the girder and there is relatively little load which can be distributed to the other girder. However, with the tuck in lane two (or three), there is considerable load distributed by the stringers and concrete deck in the longitudinal

direction. This distribution is not accounted for in the calculations using the lever rule. As a result, the calculated values would be expected to over-predict the distribution factor in the more heavily loaded girder, as confirmed by the measurements.

Longitudinal Location	Distribution Factor (%)			
	East Girder		West Girder	
	Measured	Theoretical	Measured	Theoretical
Negative Moment	3	10	97	90
Joint	10	10	90	90
Positive Moment	17	10	83	90
Average	*10*	*10*	*90*	*90*

Table 2 – Comparison of calculated and measured distribution factors for a single test truck in lane 1

Longitudinal Location	Distribution Factor (%)			
	East Girder		West Girder	
	Measured	Theoretical	Measured	Theoretical
Negative Moment	33	24	67	76
Joint	40	24	60	76
Positive Moment	38	24	62	76
Average	*37*	*24*	*63*	*76*

Table 3 – Comparison of calculated and measured distribution factors for a single test truck in lane 2

5.4.2 Effect of Transverse Position of Test Truck

Crawl tests were used to determine the general effect of transverse position of the test truck. The bottom flange stress range was compared for the east and west girders at the positive moment, joint, and negative moment locations. The bottom flange response is presented due to higher response. Figure 16 shows the girder response for the bottom flange gages in the positive moment region when the test truck was driven in the outside lanes (lanes 1 and 4).

As can be seen in Figure 16, the effect of transverse position is essentially identical in mirrored lanes. Similar results were observed for all gages installed on the main girders for all test positions. Table 4 summarizes the measured stress range for all gages installed on the main girders as the test truck crossed in each lane. It is clear from Table 4 that symmetric response was observed for all gages and all lane positions. This also confirms that superposition can be used to estimate the influence of multiple trucks on the bridge at the same time.

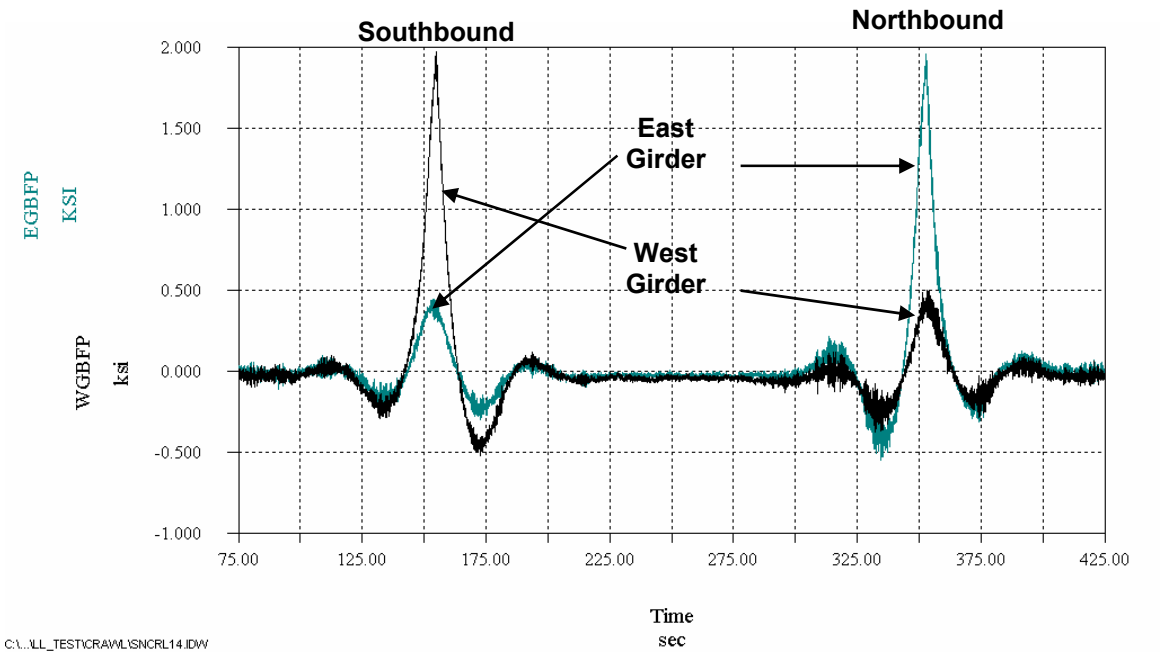

Figure 16 – Girder bottom flange response positive moment region
(truck southbound in lane 1, northbound in lane 4)

Girder	Location	Stress Range (ksi)			
		Lane 1	Lane 2	Lane 3	Lane 4
East	Positive Moment Region	0.7	1.4	2.2	2.5
West		2.5	2.1	1.4	0.9
East	Former Joint Location	0.4	0.8	1.4	1.8
West		1.7	1.3	0.8	0.4
East	Negative Moment Region	0.3	0.7	1.3	1.5
West		1.4	1.2	0.7	0.4

Table 4 – Bottom flange stress ranges measured along the girders

5.4.3 Composite Action

Initial review of the bridge showed the pre-cast deck panels attached to the girder with multiple spring clamps as shown in Figure 17. Many spring clamps were observed to be broken in the last bay near the southern abutment. The lack of connection between the deck and girder suggests that there should be little to no composite action between the deck and girders.

It is worth noting that while underneath the deck near the southern abutment, a gap of about ¼ inch was observed between the deck and the top of the top flange of the west girder. During that time a heavy truck drove over the bridge and the gap was observed to close until the deck sat on the girder. The deck then rebounded to its original position after the truck passed.

Figure 17 – Portion of bottom of deck.
Notice missing spring clamp on left

Data from the outer lane park test were used to estimate the actual degree of composite action. The data from the west girder data were used since it was located directly under the test truck. Figure 18 shows a plot of the location of the neutral axis with respect to the bottom flange of the girder at the positive moment region. Figure 18 also shows the west girder bottom flange stress response at the same location on the same time scale. The variation in bottom flange corresponds to various longitudinal positions of the test truck. As can be seen in Figure 18, the location of the neutral axis does not remain constant. Similar observations have been seen in other bridges, and is typically noted in field measurements.

The most reasonable estimate of the neutral axis can be taken at around time equal to 175 to 200 seconds. At this point, the positive moment was maximized since the bottom flange stress is greatest in the region of the plot. Varying values for neutral axes and level of composite action were also found longitudinally along the bridge. However, a reasonable location is about 85 to 90 inches above the bottom of the bottom flange. The data reported in Table 5 are the locations of the neutral axis at the maximum positive bottom flange west girder response. Also presented in Table 5 is the theoretical location of the neutral axis assuming both non-composite and fully composite action. The data suggest that the girders are highly composite in the regions instrumented.

Most interesting are the data collected near the location of the former pin and hanger. The measurements seem to over-predict the level of composite action considerably. The exact reason for this is not clear but likely related to the dual floorbeams at this location and additional lateral bracing. These members will influence the stress distribution in the girder at this location and tend to alter the position of the neutral axis.

The significant composite action is primarily attributed to the bond between the concrete and the riveted top flange. Field instrumentation of highway bridges consistently demonstrates that non-composite bridges act nearly fully composite under service loads. As a result, actual live load stress ranges are often much less than calculated using simple analytical models assuming non-composite behavior.

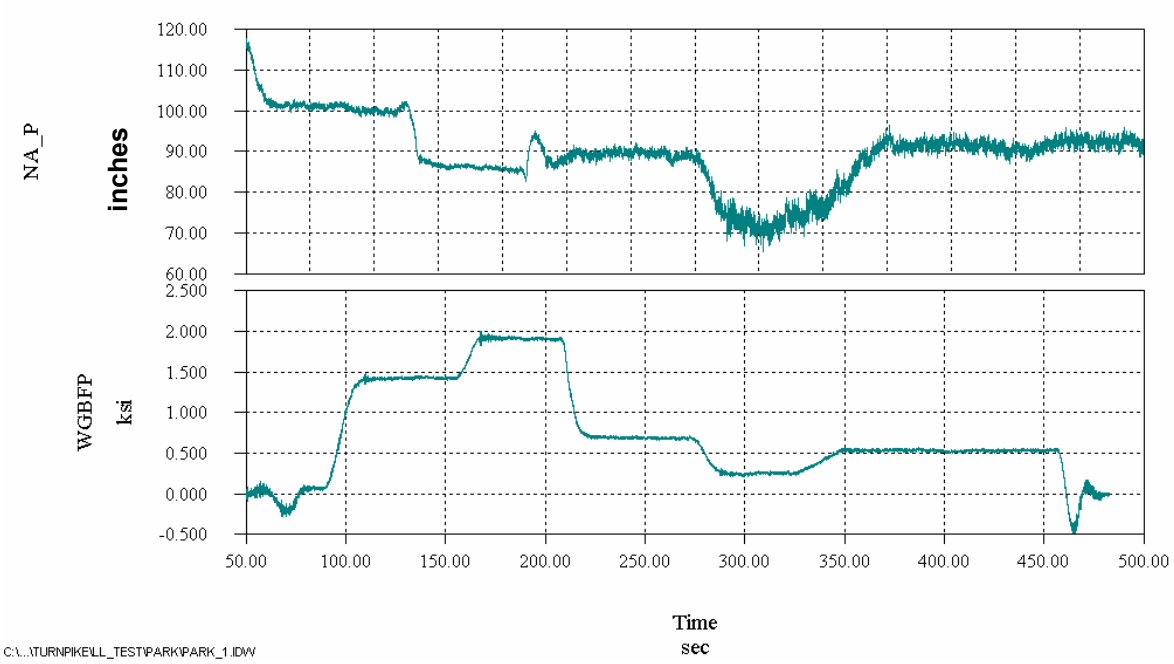

Figure 18 – Variation of neutral axis with longitudinal position of test truck at positive moment section of west girder

Longitudinal Girder Location	Calculated Neutral Axis (in)	Theoretical Neutral Axis (in)		Percent Composite (%)
		Composite	Non-composite	
Negative Moment	92 -100	93	67	103
Joint	117 - 122	93	67	128
Positive Moment	85-90	96	67	91

Table 5 – Comparison of measured and calculated neutral axis positions (measured from bottom of bottom flange)

5.4.4 Comparison of Analytical Model and Experimental Results

An influence line generated by SAP was scaled and compared with the influence line obtained from the field tests. Figure 19 shows the comparison of the analytical model to the southbound crawl test for the west girder bottom flange gage in the positive moment region.

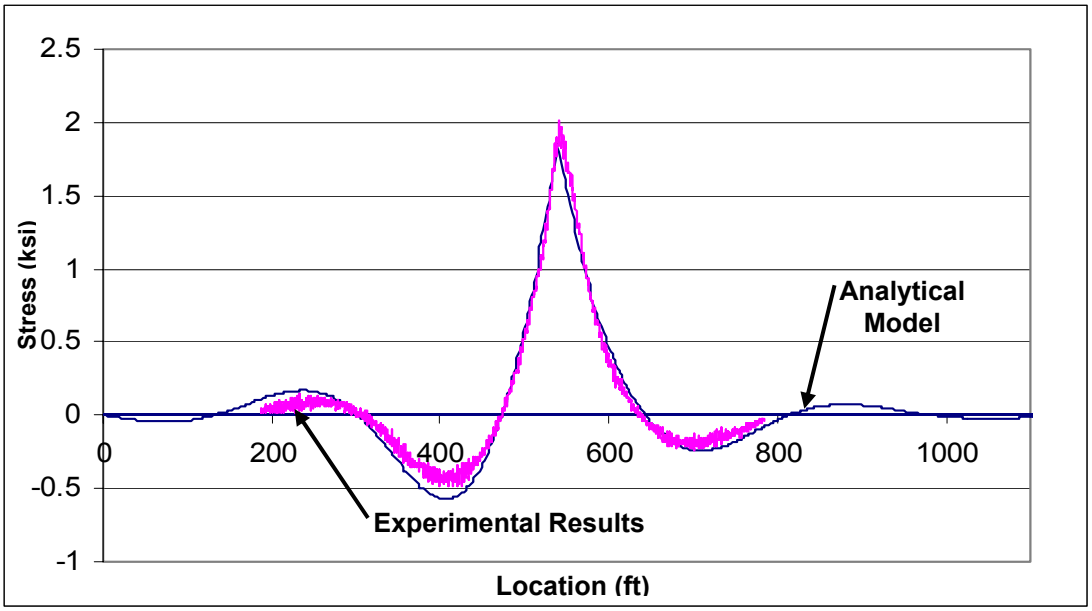

Figure 19 – Comparison of measured and calculated influence lines comparison

The SAP model was originally in terms of moment and distance from the point load to the start of the bridge, while the field data was in terms of stress and time elapsed. The model was scaled using the stress-moment relationship: $S = Mc / I$, where M is the moment, c is the distance from the gage to the neutral axis, and I is the moment of inertia. A scale factor was also necessary to convert the two-dimensional SAP model to something equivalent to one of the girders of the existing bridge. The load distribution factor found with the lever rule for an outside lane test was applied to calculated values from SAP. A final scale factor was needed to convert the one-kip moving point load used in SAP to the 62.4 kip truck used in the live load tests. The results of the scaled influence line correlate very well to the obtained field results, as shown in Figure 19. Table 6 shows this correlation.

	Maximum Stress (ksi)	Minimum Stress (ksi)
Measured Stress (ksi)	2.0	-0.5
Calculated Stress (ksi)	1.9	-0.6

Table 6 – Comparison measured and calculated minimum and maximum stresses

5.4.5 Floorbeam Response

As discussed, gages were installed on the bottom of the top flange and bottom of the bottom flange of the floorbeam located near location of the former pin and hanger location. Gages were located on the floorbeam near midspan and near the connection to the west girder. As expected, significant stresses are only produced in the floorbeam when vehicles travel in lanes two and three. Trucks crossing in lanes one or four are essentially located directly over the main girders and do not place any significant load in the floorbeam. This is illustrated in Figure 20 which compares the response of the bottom flange at midspan for trucks traveling in lanes 1 and 2.

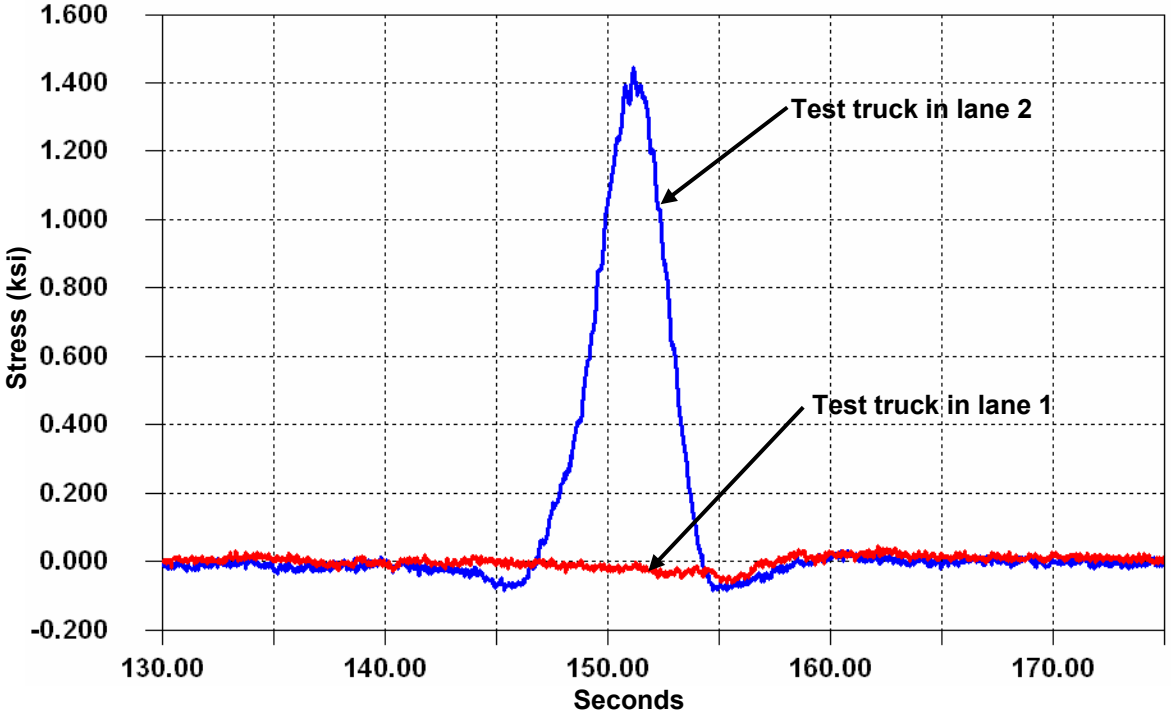

Figure 20 – Comparison of floorbeam bottom flange response at midspan as test truck passed in lane one and lane two

It is clear from Figure 20 that the test truck produced no effect when passing in lane 1. However, as expected, the bottom flange was subjected to measurable tensile stress as the truck passed in lane 2. As stated, similar results were obtained as the truck passed in lanes 3 and 4.

Figure 21 compares the response of the top and bottom flange of the floorbeam as the test truck passed in lane two. As expected, the top and bottom flanges are in compression and tension respectively. The top flange of the floorbeam is not embedded in the deck slab, hence the stresses would be expected to be equal and opposite. However, there are local effects which are the result of the point loads applied by the stringers which are near the top flange gage. In addition, the top flange gages were located on the bottom of the top flange and would be subjected to lower stresses than on the top of the top flange.

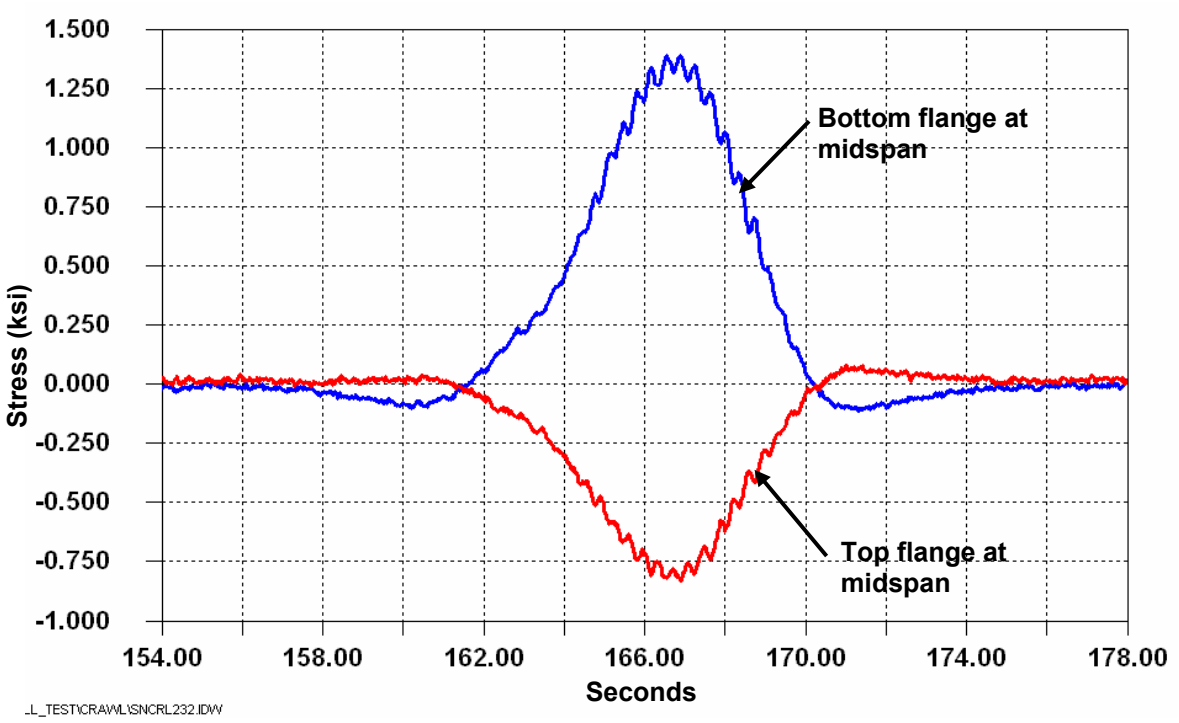

Figure 21 – Response of top and bottom flange of floorbeam at midspan as test truck passed in lane 2

5.5 Stringer Response

Strain gages were installed at midspan of the first interior stringer near the west girder. Gages were located on the bottom of the bottom flange and on the bottom of the top flange. Measurable stresses were only observed as the test truck passed in lane 1 or 2. Very little stress was produced as the truck passed in lanes 3 or 4, as expected. Stringers are very sensitive to the transverse position of wheel loads. When the truck is in lane two, the right wheels are nearly directly over the stringer. Hence, the greatest stresses are produced (*in this stringer*) with the trucks in this lane.

The response of the stringer to the front axle and rear axles is also clearly distinguished in Figure 22. In fact, the response of the rear axles (i.e., tandem) is discernable in the top flange response as the truck passed in lane 2. In addition, the response of the top flange is less than measured in the bottom flange. However, it must be noted that the top flange gages were installed on the bottom of the top flange which is not the location of maximum compressive stress. However, the magnitude of the difference suggests that a certain level of composite action exists between this stringer and the deck.

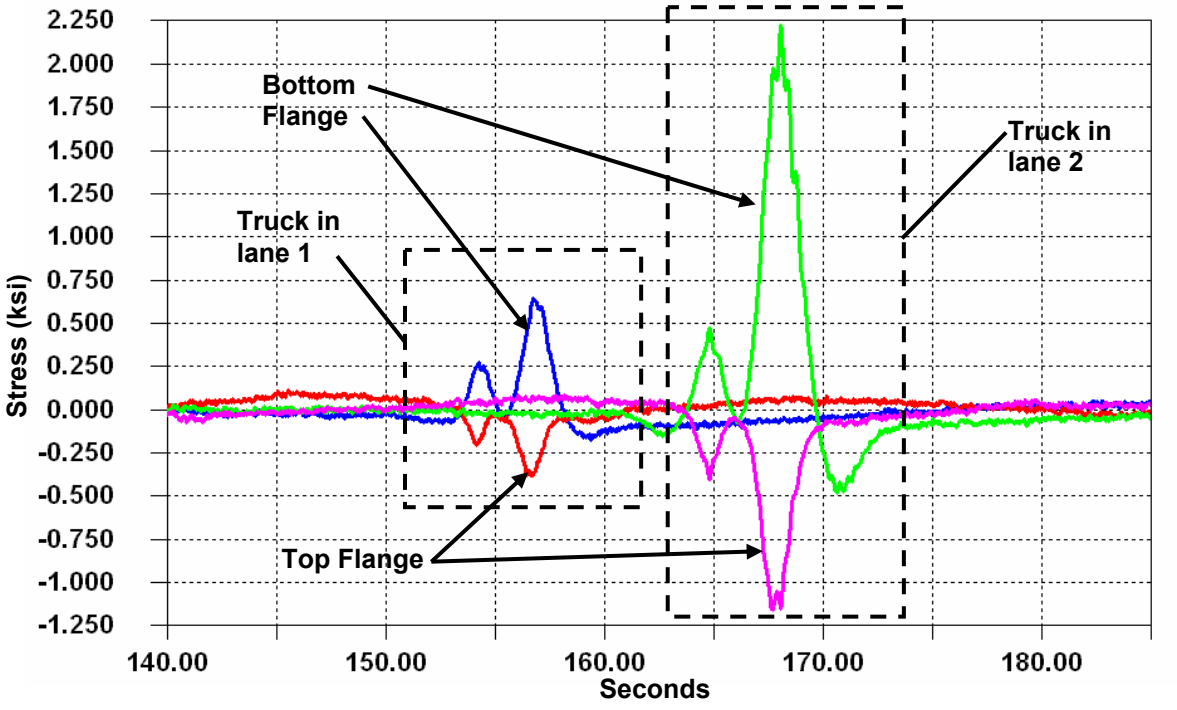

Figure 22 – Stringer response as test truck passed in lanes 1 and 2

6.0 Results of Uncontrolled Monitoring

All gages were monitored for a total of six days and 22.5 hours beginning on July 11, 2003. During this time, triggered time history data were recorded and stress-range histograms were developed at all gages. As mentioned, the time history data were recorded only when stresses at selected locations (*i.e., gages*) exceeded predefined stress magnitudes. The gages selected as the "trigger" channels were located on the bottom flange of the east and west girders at midspan of span four.

Figure 23 presents a selected portion of the triggered time history data collected during three monitoring period as random trucks crossed the bridge. The data are from the bottom flange of the west girder in the positive moment region. Notice that although the events appear equally spaced, they actually occur hours apart, since these are only triggered events.

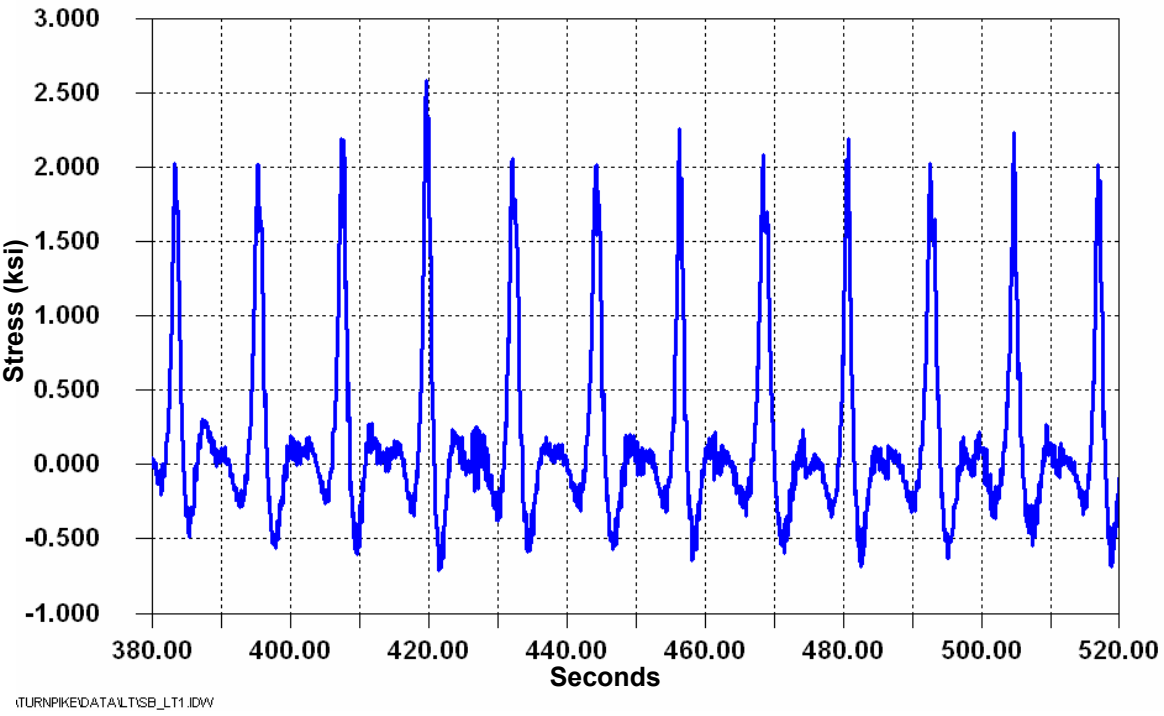

Figure 23 – Selected portion of the typical triggered time history data from bottom flange positive moment region of the west girder in span four (trucks headed southbound)

One of the largest stress ranges measured in the main girders is presented in Figure 24. These data were recorded during a southbound trigger event. It is thought to been produced by a single truck with a heavy trailer or two trucks nearly side-by-side (i.e., in lanes one and two) passing at the same instant. Although this is the largest stress range observed in the time history data, the peak-to-peak stress range is only about 4.1 ksi in the bottom flange of the west main girder.

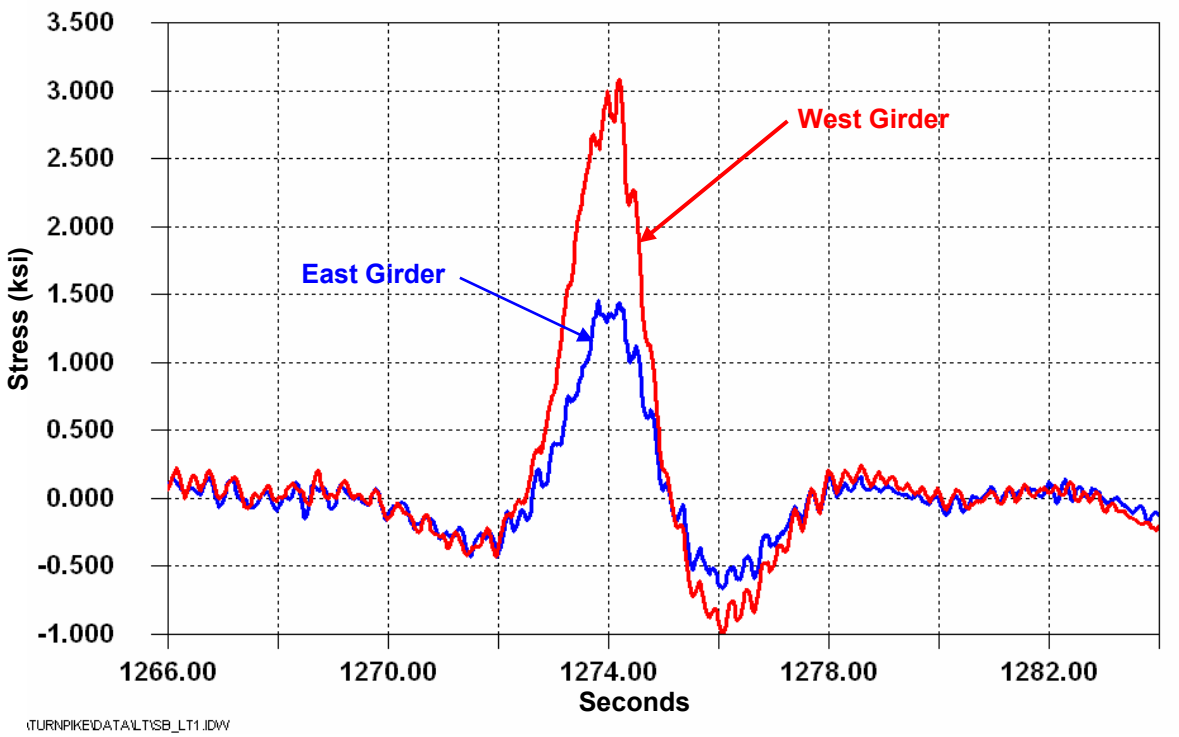

Figure 24 – Maximum random stress range observed in bottom flange of west girder at midspan of span four (*East girder response shown for information)*

6.1 Stress-Range Histograms

Stress-range histograms were developed for all gages and are summarized in Table 7. Effective stress ranges (S_{reff}) were calculated ignoring all cycles less than 1.0 ksi, which is a reasonable cutoff threshold for these details. (*The effective stress range is intended to represent the equivalent cumulative damage of a variable amplitude stress-range spectrum.*) As can be seen, no stress range cycle (i.e., S_{rmax}) exceeded the constant amplitude fatigue limit of any of the details. Hence, infinite life is expected in the areas where instrumentation was installed. Assuming the stress-range histograms are is representative of the rest of the bridge and over the life of the structure, fatigue due to primary stresses would not be expected in this structure.

Channel	S_{reff}	S_{rmax}	Total Cycles	Cycles per Day	Category (CAFL)	Fatigue Life
EGTFN	1.2	1.5	351	51	D (7.0ksi)	*Infinite*
EGBFN	1.4	2.5	4,054	584	D (7.0ksi)	*Infinite*
EGTFJ	***See Note 1***				D (7.0ksi)	*Infinite*
EGBFJ	1.5	3.0	3,990	575	D (7.0ksi)	*Infinite*
EGTFP	1.3	2.0	1,217	175	D (7.0ksi)	*Infinite*
EGBFP	1.8	4.0	6,462	931	D (7.0ksi)	*Infinite*
WGBFP	2.0	5.0	5,865	845	D (7.0ksi)	*Infinite*
WGTFP	1.4	3.0	2,217	320	D (7.0ksi)	*Infinite*
WGBFJ	1.7	3.0	3,459	499	D (7.0ksi)	*Infinite*
WGTFJ	***See Note 1***				D (7.0ksi)	*Infinite*
WGBFN	1.4	3.0	4,475	645	D (7.0ksi)	*Infinite*
WGTFN	1.3	2.5	96	14	D (7.0ksi)	*Infinite*
WFBBF	1.2	1.5	102	15	D (7.0ksi)	*Infinite*
WFBTF	1.3	2.0	286	41	D (7.0ksi)	*Infinite*
CFBBF	1.3	2.0	230	33	D (7.0ksi)	*Infinite*
CFBTF	1.2	1.5	37	5	D (7.0ksi)	*Infinite*
STRBF	1.7	4.0	4,994	720	A (24.0ksi)	*Infinite*
STRTF	1.3	2.0	1,965	283	A (24.0ksi)	*Infinite*

Notes

1. No stress range cycles greater than 1.0 ksi were measured.

Table 7 – Summary of stress-range histograms determined for the entire monitoring period (July 11-17, 2003)

7.0 Conclusions

The Clarks Summit Bridge was found to act continuously with a full moment reaction at each of the former pin and hanger joint locations. It was also found to behave with a relatively high level of composite action in areas where instrumentation was installed.

The average factor for stress distribution between girders matches well with the theoretical stress distribution factor when the truck is in lanes 1 and 4, as seen in Table 2. However, when the truck is in lanes 2 or 3, the average stress distribution factor does not correlate with the theoretical distribution factor, as seen in Table 3. This is likely due to greater load distribution in the longitudinal direction.

Transverse truck position resulted in a mirrored effect in opposite lanes, as seen in Table 4 and Figure 16. This is to be expected as the floorbeam should be able to distribute load regardless of the origin of the load.

A comparison between an influence line created analytically with SAP 2000 and an influence line obtained experimentally from the same longitudinal location showed that the model and the field data were close enough to assume that the pin and hanger model is an accurate representation of the behavior of the bridge both before and after the retrofit of the pin and hanger connections.

Stress-range histograms were developed over a period of almost seven days. None of the stress-range cycles exceeded the CAFL of the fatigue details near the instrumented sections, which were primarily category D details (CAFL for category D is 7.0 ksi). The effective stress range (S_{reff}) was well below the CAFL of all details near the instrumented portions of the bridge. Assuming that truck loading has been reasonable similar to that observed curing the monitoring program and that the measurements are representative of the rest of the structure, no fatigue cracking as a result of primary stresses are anticipated.

8.0 Acknowledgments

This work was sponsored by the Pennsylvania Infrastructure Technology Alliance (PITA), the Pennsylvania Turnpike Commission, and the ATLSS Engineering Research Center at Lehigh University. Special thanks are due to the PA Turnpike Commission for their support by providing all traffic control, access equipment, and the test truck throughout the research. The efforts of Mr. Bernie J. Zielinski, P.E. and Mr. William Barnhart of the Pennsylvania Turnpike Commission are greatly appreciated by the authors.

9.0 References

1. National Transportation Safety Board. July 1984 "Highway Accident Report – Collapse of a Suspended Span of Interstate Route 95 Highway Bridge over the Mianus River. Greenwich, CT June 28 1983." Washington, D.C. United States Government.

2. Yen, Ben T. et al. Jan. 1990 Manual for Inspecting Bridges for Fatigue Damage Conditions. . Bethlehem, PA. Lehigh University

3. Christie, Scott and John M. Kulicki. Feb. 1991 "New Support for Pin and hanger Bridges." Civil Engineering-ASCE. Vol. 61 no. 2. p.62-64.

4. Ghosn, Michel and Fred Moses. Aug.1995 "Redundancy in Highway Bridge Superstructures." Fourth International Bridge Engineering Conference. Vol. 2. San Francisco, CA. Transportation Research Board and National Research Council.

5. American Institute of Steel Construction, Inc. 1959 Moments, Shears and Reactions: Continuous Highway Bridge Tables. New York, NY.

APPENDIX A:

INSTRUMENTATION PLANS

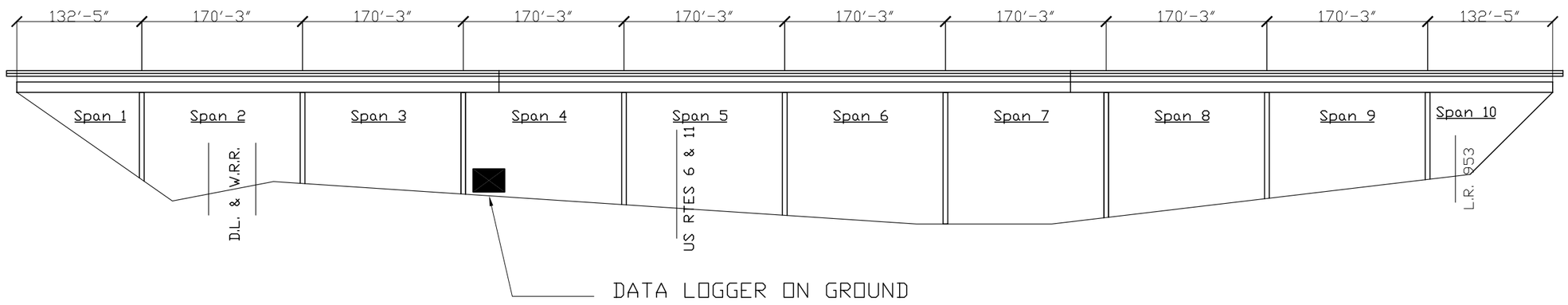

ELEVATION

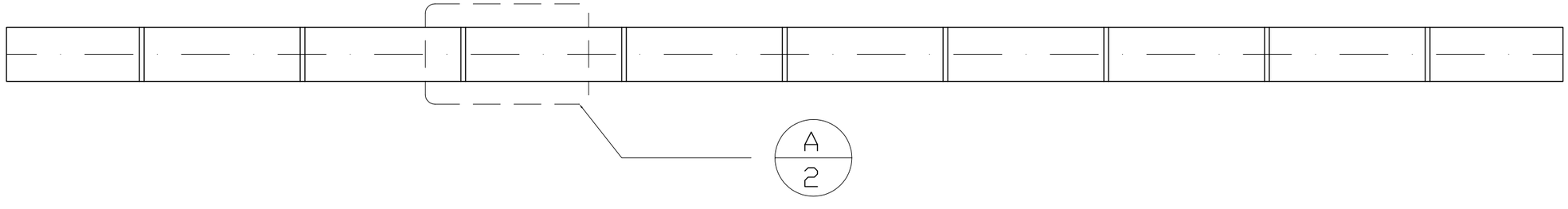

PLAN

ATLSS
ADVANCED TECHNOLOGY FOR
LARGE STRUCTURAL SYSTEMS
117 ATLSS Drive
Lehigh University
Bethlehem, PA 18015
610-758-3500 FAX 610-758-5553

PROJECT:

Clarks Summit Bridge

SHEET NOTES:

NO.	DESCRIPTION	DATE	BY
2	FINAL	2/4/04	ICH
1	INITIAL SUBMITTAL	6/24/03	BHW

DESIGNED BY:	BHW/RJC
DRAWN BY:	BHW
CHECKED BY:	RJC/ICH
SCALE:	N.T.S
DATE:	6/24/03
PROJECT NO.:	REU PROJECT

SHEET TITLE:

ELEVATION AND PLAN VIEWS

SHEET NO.:

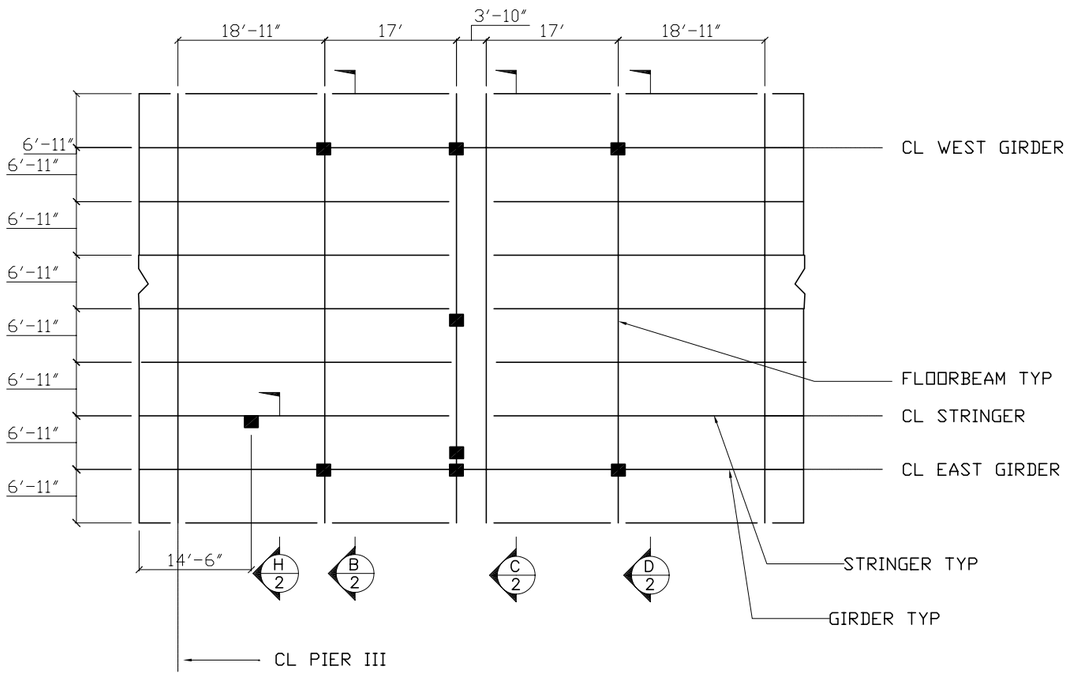

DETAIL A

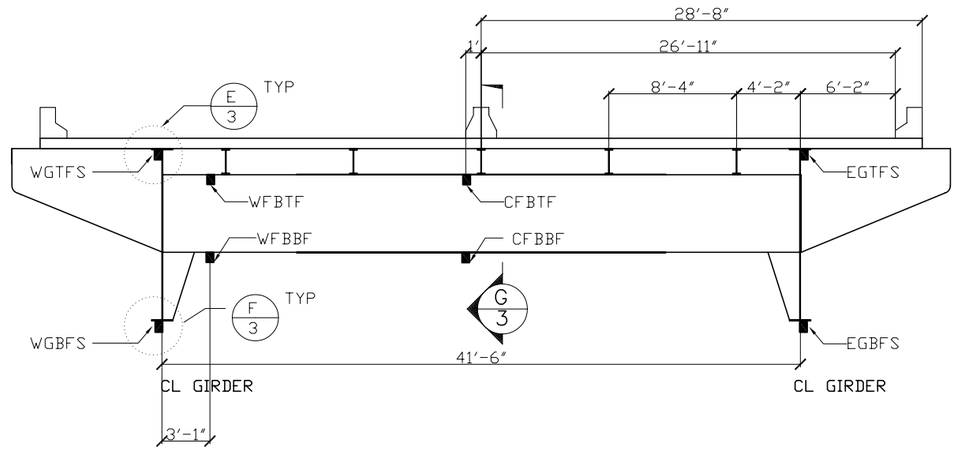

DETAIL B

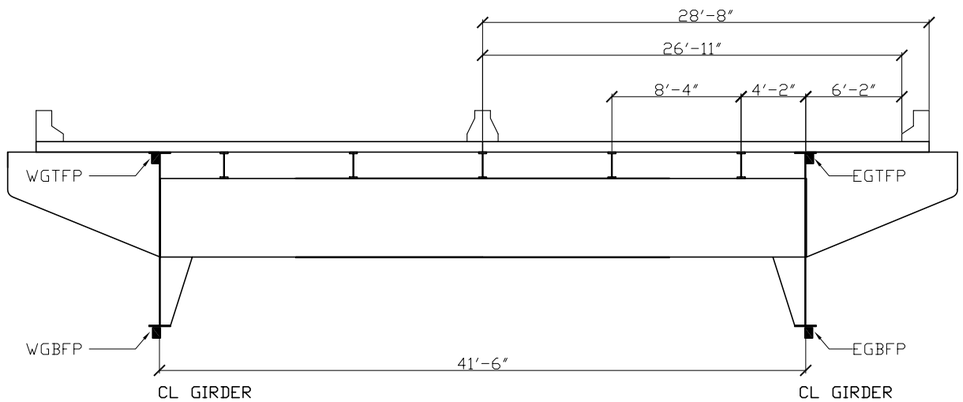

DETAIL C

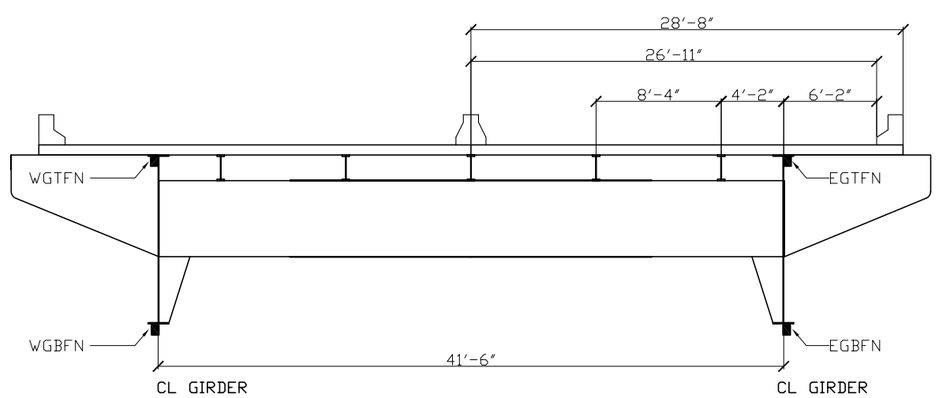

DETAIL D

ATLSS
ADVANCED TECHNOLOGY FOR
LARGE STRUCTURAL SYSTEMS
117 ATLSS Drive
Lehigh University
Bethlehem, PA 18015
610-758-3500 FAX 610-758-5553

PROJECT:

Clarks Summit Bridge

SHEET NOTES:

NO.	DESCRIPTION	DATE	BY
2	FINAL	2/4/04	RJC
1	INITIAL SUBMITTAL	6/24/03	BHW

DESIGNED BY:	BHW/RJC
DRAWN BY:	BHW
CHECKED BY:	RJC/ICH
SCALE:	N.T.S
DATE:	6/24/03
PROJECT NO.:	REU PROJECT

SHEET TITLE:

SECTIONS AND DETAILS

SHEET NO.:

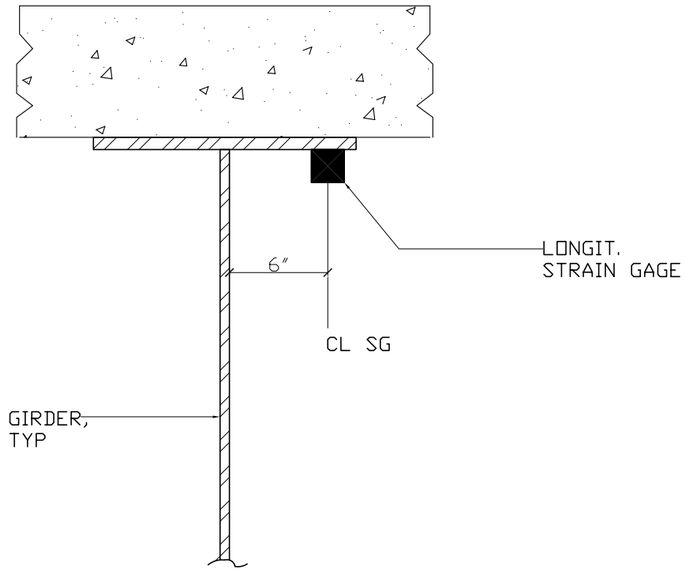

DETAIL E

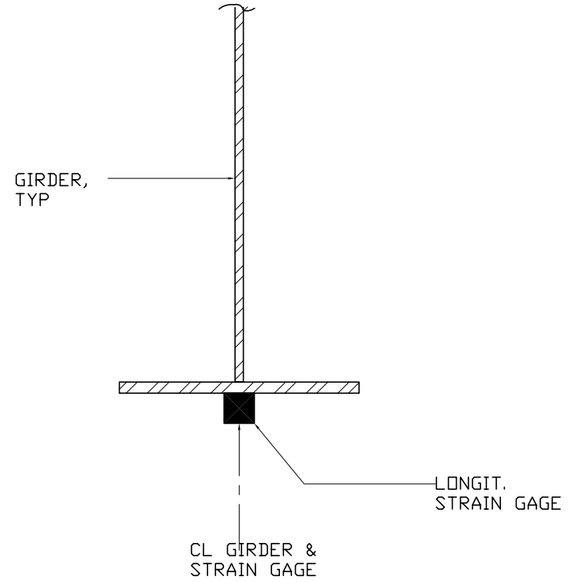

DETAIL F

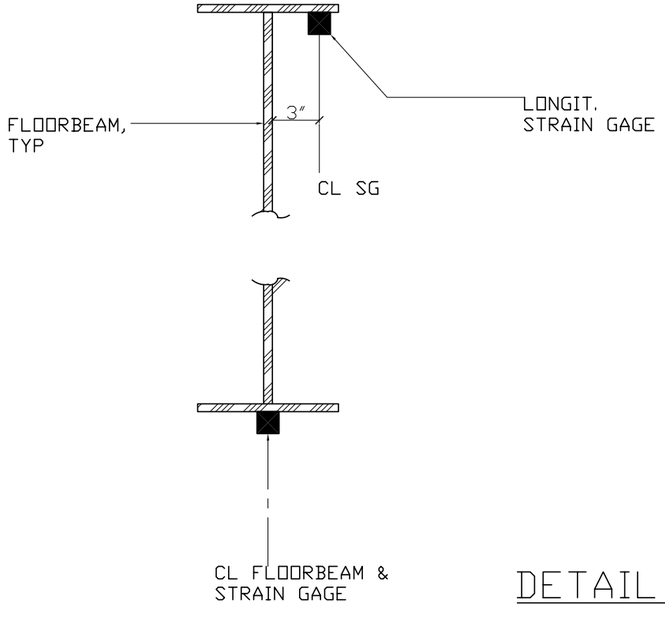

DETAIL G

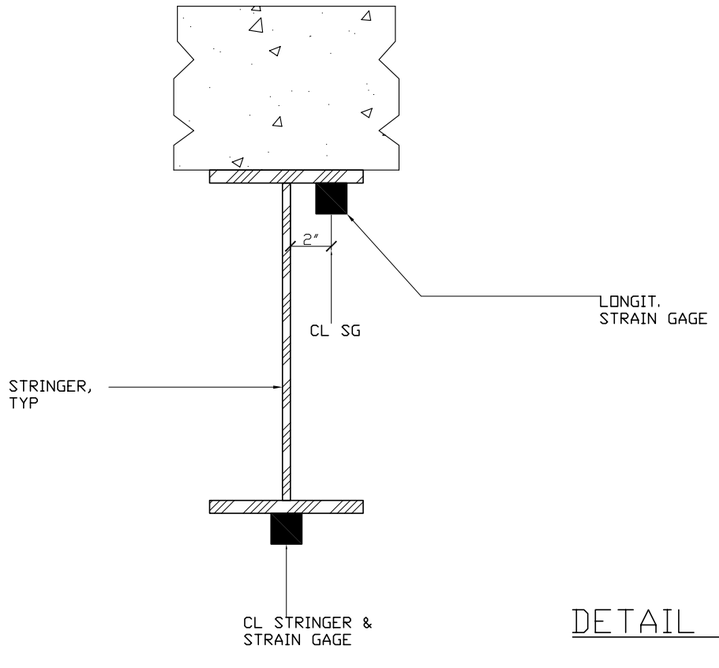

DETAIL H

ADVANCED TECHNOLOGY FOR
LARGE STRUCTURAL SYSTEMS
117 ATLSS Drive
Lehigh University
Bethlehem, PA 18015
610-758-3500 FAX 610-758-5553

PROJECT:

Clarks Summit Bridge

SHEET NOTES:

NO.	DESCRIPTION	DATE	BY
2	FINAL	2/4/04	RJC
1	INITIAL SUBMITTAL	6/24/03	BHW

DESIGNED BY:	BHW/RJC
DRAWN BY:	BHW
CHECKED BY:	RJC/ICH
SCALE:	N.T.S
DATE:	6/24/03
PROJECT NO.:	REU PROJECT

SHEET TITLE:

SECTIONS AND DETAILS

SHEET NO.:

3 OF 3